

# Ultra-deep-subwavelength Light Transport in Hybrid Nanowire-loaded Silicon Nano-rib Waveguides

Qiang Ren, Yusheng Bian, Ping Werner and Douglas Werner\*  
 Computational Electromagnetics and Antennas Research Lab (CEARL)  
 Department of Electrical Engineering, The Pennsylvania State University  
 University Park, PA, 16802, USA  
 \*dhw@psu.edu

**Abstract**—We report a high-performance silicon-based hybrid plasmonic waveguide that consists of a silicon nano-rib loaded with a metallic nanowire. An ultra-deep-subwavelength mode area ( $\lambda^2/4.5 \times 10^5 \sim \lambda^2/7 \times 10^3$ ), in conjunction with a reasonable propagation distance (2.2 ~ 60.2  $\mu\text{m}$ ), is achievable at a telecommunication wavelength of 1.55  $\mu\text{m}$ , which indicates that this device outperforms its conventional hybrid and nanowire waveguiding counterparts.

**Keywords**—Hybrid waveguide; Nanowire; Silicon-on-insulator

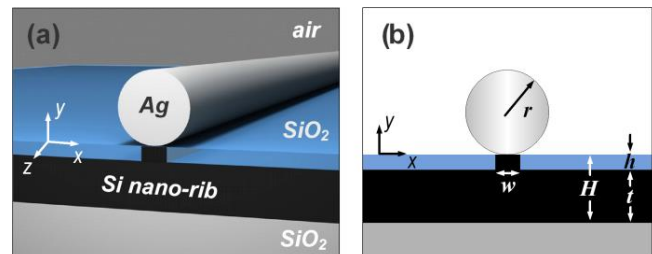
## I. INTRODUCTION

As an emerging field in nanophotonics, hybrid plasmonic waveguides (HPWs) that integrate plasmonic configurations and high-index dielectric structures have recently received significant attention owing to their remarkable capability of simultaneously enabling subwavelength field confinement and long-range propagation [1, 2]. Numerous high-performance integrated photonic components have been developed based on such a hybrid platform [2]. Moreover, the original hybridization concept has been extended to a number of other configurations as well [2-6]. Although various alternative hybrid guiding structures have been proposed during recent years, most of these modified waveguides are still subject to certain limitations: some of them suffer from the tradeoff between modal attenuation and field localization, while others face significant challenges for practical applications due to the additional fabrication complexities introduced in the design. Here, by combining a metallic nanowire (NW) with a Si nano-rib, we present a simple and feasible approach to improve the optical performance of HPWs. Owing to the efficient hybridization of the NW plasmon polariton and the Si nano-rib waveguide mode, our proposed hybrid waveguide features an extremely small mode size (down to the ultra-deep-subwavelength scale), while maintaining reasonable propagation distance at telecommunication wavelengths.

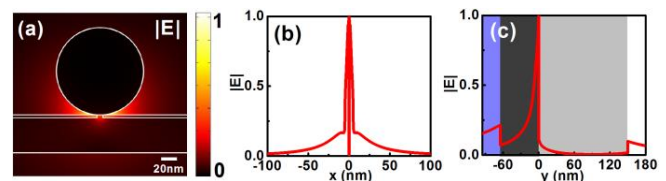
## II. WAVEGUIDE GEOMETRY AND MODAL PROPERTIES

Fig. 1 shows schematically the geometry of the hybrid NW-loaded Si nano-rib structure, which consists of a metallic NW sitting on top of a Si nano-rib waveguide, with a thin silica layer coating on the Si slab. Due to the unique waveguide configuration, a hybrid, non-uniform gap is formed between the upper metal NW and the lower Si substrate, which greatly facilitates the coupling between the NW plasmon and Si

photonic modes. In the following, the waveguide properties are investigated numerically by solving the Helmholtz equation using the eigenmode solver of the finite element method (FEM) based software COMSOL<sup>TM</sup> with a scattering boundary condition. The refractive indices of SiO<sub>2</sub>, Si, air and Ag at an operating wavelength of 1550 nm are taken as  $n_s = 1.444$ ,  $n_d = 3.476$ ,  $n_c = 1$  and  $n_m = 0.1453 + 14.3587i$  [1], respectively. Without loss of generality, a rectangular-shaped silicon nano-rib is chosen as a proof-of-concept, while our studies show that the waveguide concept presented here can also be applied to many other configurations with similar nanostructures.



**Fig. 1.** Hybrid NW-loaded Si nano-rib waveguide. (a) Schematic of the three-dimensional (3D) geometry; (b) Cross-section of the configuration. The waveguide comprises a silver NW (with a radius of  $r$  and a refractive index of  $n_m$ ) located above a Si nano-rib structure (with a refractive index of  $n_d$ ) over a silica substrate (with a refractive index of  $n_s$ ). An additional silica buffer layer (with a height of  $h$ ) is sandwiched between the NW and the Si slab. The height of the Si waveguide is  $H$  and the rib width is  $w$ . The NW is positioned at the center (along  $x$  axis) with respect to the Si nano-rib.



**Fig. 2.** Normalized electric field distributions of the fundamental hybrid plasmonic mode supported by the proposed waveguide. (a) 2D field profile; (b)-(c) 1D field plots along  $x$  and  $y$  directions. The geometric parameters of the waveguide were chosen as:  $w = 10$  nm,  $h = 5$  nm,  $r = 75$  nm,  $t = 60$  nm. The 1D field profiles are taken at the bottom corner of the Ag NW.

Normalized electric field distributions of the fundamental plasmonic mode supported by a typical hybrid waveguide are shown in Fig. 2. Significant local field enhancements along both the horizontal and vertical directions can be observed

This work was partially supported by the Penn State MRSEC, Center for Nanoscale Science, under the award NSF DMR-1420620.

inside the nanoscale, hybrid gap region, which is quite beneficial for achieving ultra-tight field confinement. By tuning key structural parameters of the waveguide, the hybridization of the NW plasmon and Si photonic modes can be regulated, leading to varied modal properties shown in Fig. 3. The definitions of modal effective index ( $n_{eff}$ ), propagation length ( $L$ ), normalized mode area ( $A_{eff}/A_0$ ), confinement factor ( $\Gamma_{gap}$ ,  $\Gamma_{Si}$ ) and figure of merit ( $FoM$ ) are the same as those reported in [6]. To ensure moderate propagation loss, ultra-deep-subwavelength mode size and reasonable confinement inside the gap and Si waveguide region,  $w$  and  $h$  are fixed at 10 nm and 5 nm, respectively, whereas  $r$  is varied between 10 nm and 80 nm, along with different slab thickness (20 nm, 40 nm, 60 nm). As illustrated in Fig. 3, due to the gradually enhanced field confinement, increased  $n_{eff}$ , reduced  $A_{eff}$  and decreased  $L$  are all observable for waveguides with different slab thicknesses when the NW becomes smaller. Within the considered parameter range, the mode sizes of the hybrid nano-rib waveguide can be maintained at the ultra-deep-sub-wavelength scale, which are much smaller than its conventional HPW and nanowire-over-substrate (NWOS) counterparts. Ultra-small mode area ( $A_{eff}/A_0$ :  $8.9 \times 10^{-6} \sim 5.7 \times 10^{-3}$ ) and reasonable propagation distance ( $L$ : 2.2 to 60.2  $\mu\text{m}$ ) can be achieved simultaneously. In addition, our calculations reveal that the ratios of the modal power residing in the hybrid gap region and the silicon nano-rib structure are also higher than those achieved by the conventional HPW [1] and NWOS configurations [4].

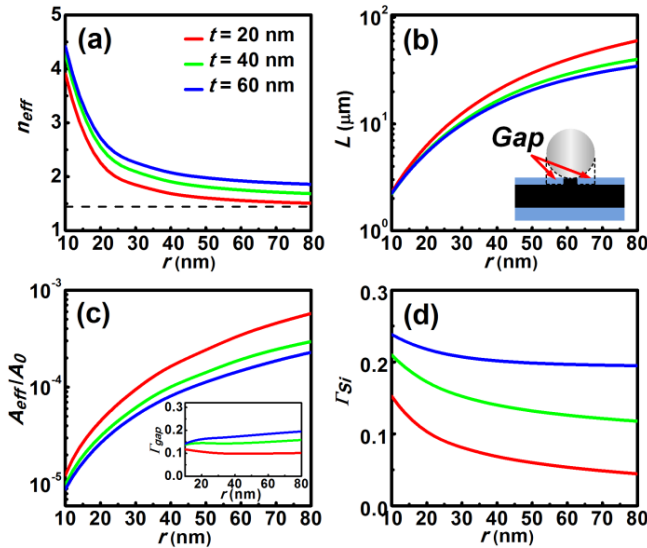


Fig. 3. Dependence of modal properties on the radius of the silver NW for a Si slab with different thickness ( $w = 10$  nm,  $t = 5$  nm): (a)  $n_{eff}$ ; (b)  $L$ , inset showing schematically the gap region in the study; (c)  $A_{eff}/A_0$ , where the inset shows the result of  $\Gamma_{gap}$ ; (d)  $\Gamma_{Si}$ . The dashed black line in (a) corresponds to the refractive index of the  $\text{SiO}_2$  substrate ( $n_s = 1.444$ ).

By performing 2D parametric studies of normalized mode area versus normalized propagation length, we are able to further benchmark the performance of the proposed hybrid waveguide. Comparisons between its guiding properties and those of a conventional metallic NW (bare metallic NW in an air cladding) and a HPW (Si NW placed near a silver substrate)

reveal that, for similar propagation distances, the mode area of the hybrid NW-loaded Si nano-rib waveguide can be 1~2 orders of magnitude smaller than those of its conventional hybrid/NW counterparts, as illustrated in Fig. 4. The proposed waveguide also features a significantly higher  $FoM$  than conventional NW, HPW and NSOW structures, which further confirms its superior guiding properties. In addition, our studies indicate that the optical performance of the proposed waveguide is also highly tolerant to possible fabrication imperfections, such as the misalignment between the upper NW and the lower nano-rib, which renders it a promising candidate for practical implementation.

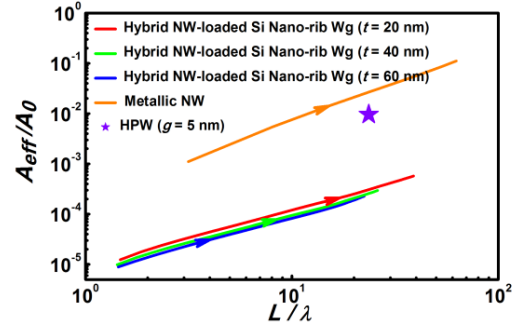


Fig. 4. Parametric plots of normalized mode area ( $A_{eff}/A_0$ ) versus normalized propagation length ( $L/\lambda$ ). A trajectory corresponds to a range of NW radius:  $r = [10, 80]$  nm. Arrows indicate increasing the size of the NW. The dimension of the HPW is  $r = 100$  nm and  $g = 5$  nm [1]. To allow fair comparisons, the refractive indices of the materials for all waveguides are the same.

### III. CONCLUSION

In summary, we have developed a high-performance HPW by integrating a metallic NW with a Si nano-rib configuration. The mode area of the waveguide is 1~2 orders of magnitude smaller than those of the conventional HPW and metallic NW configurations with similar propagation distances. Our proposed hybrid waveguiding structure offers good compatibility with Si-on-insulator platforms and could be a promising building block for ultra-compact passive and active integrated photonic components.

### REFERENCES

- [1] R. F. Oulton, *et al.*, "A hybrid plasmonic waveguide for subwavelength confinement and long-range propagation," *Nat. Photon.*, vol. 2, pp. 496-500, 2008.
- [2] M. Z. Alam, *et al.*, "A marriage of convenience: Hybridization of surface plasmon and dielectric waveguide modes," *Laser Photonics Rev.*, vol. 8, pp. 394-408, 2014.
- [3] D. X. Dai and S. L. He, "A silicon-based hybrid plasmonic waveguide with a metal cap for a nano-scale light confinement," *Opt. Express*, vol. 17, pp. 16646-16653, Sep 2009.
- [4] S. P. Zhang and H. X. Xu, "Optimizing substrate-mediated plasmon coupling toward high-performance plasmonic nanowire waveguides," *Acc Nano*, vol. 6, pp. 8128-8135, Sep 2012.
- [5] Y. S. Bian and Q. H. Gong, "Low-loss light transport at the subwavelength scale in silicon nano-slot based symmetric hybrid plasmonic waveguiding schemes," *Opt. Express*, vol. 21, pp. 23907-23920, Oct 2013.
- [6] Y. S. Bian and Q. H. Gong, "Metallic-nanowire-loaded silicon-on-insulator structures: A route to low-loss plasmon waveguiding on the nanoscale," *Nanoscale*, vol. 7, pp. 4415-4422, 2015.